

for advertising or promotional purposes or for creating new collective works for resale or redistribution to servers or lists, or to reuse any copyrighted component of this work in other works must be obtained from the IEEE.

## THE DESIGN OF THE ISR INFLECTOR

by

H. Kuhn, W. C. Middelkoop and H. O'Hanlon

CERN, Geneva, Switzerland.

### Summary

Protons with momenta up to 28 GeV/c will be ejected from the CERN Proton Synchrotron (CPS) transferred via two beam transfer channels, each about 500 m long and injected into each of the two Intersecting Storage Rings (ISR) which are being constructed at CERN. At  $1/4$  betatron wavelength downstream of the injection septum magnet a fast pulsed inflector deflects the beam over an angle of 2.5 mrad onto the injection orbit. This pulsed inflector consists of two delay-line type magnets each 1.5 m long, which operate in ultra high vacuum. The C-shaped ferrite magnets have a gap width of 44.5 mm and a gap height of 20 mm. The useful magnetic field region is more than 40 mm wide.

A prototype inflector has been constructed with all auxiliary electrical elements, one magnet and two UHV tanks. The 2.1  $\mu$ sec long magnetic pulses are generated by discharging a coaxial high voltage cable via a deuterium thyratron into the magnet and its matched terminating resistor of  $14 \Omega$ . The droop on the magnetic field flat top is 1% and the transients on the flat top and at 1  $\mu$ sec after the pulse are within  $\pm 1\%$ . The magnet has been tested at its maximum required operating voltage of 21.5 kV and, additionally, at 25 kV in a vacuum of  $10^{-10}$  torr.

### Introduction

This paper concerns the design, construction and results obtained with a prototype fast inflector magnet of the same design as those that will be used for inflecting the proton beam onto its injection orbit in each of the rings of the ISR in a single turn injection process after its transfer from the CPS.<sup>1</sup> As such, these magnets are in principle equivalent to the fast ejection system of a 28 GeV Synchrotron.

Figure 1 shows the use of the nominal ISR aperture of 150 mm for the injected beam and a stacked beam of 2% momentum spread at an azimuthal position of maximum horizontal beam size which corresponds approximately to the inflector position.

The injected beam will continue to circulate around the ring on the injection orbit passing through the gap of the inflector magnet until it is accelerated towards the stack. This implies that the inflector magnetic field must be reduced to zero before the protons, after the first revolution, pass through the gap again. In the CPS the harmonic number is 20 and the beam revolution time is 2.1  $\mu$ secs. The ISR diameter will be  $3/2$  times that of the CPS. Therefore, the ISR has an harmonic number of 30 and a beam revolution time of 3.15  $\mu$ sec. Only 20 out of the 30 ISR

buckets will be filled before stacking, the remaining 10 empty buckets being suppressed in order not to dilute the phase space density of the stacked beam.<sup>2</sup> It follows that the magnetic pulse of the inflector must have a 2.1  $\mu$ sec flat top and the fall time to zero must be within the ensuing 1.05  $\mu$ secs. The logical choice of magnet type for this application is a small aperture C-shaped magnet operating inside the ultra high vacuum chamber.

Also shown in Fig. 1 is an aluminium alloy screen which prevents the already stacked beam from being perturbed by the stray field of the pulsed inflector. The screen will be driven in a rotary sense such that the gap is closed by it during pulsing of the inflector and opened during stacking when the beam traverses the gap from the injection orbit towards the stacked beam position. When stacking has been completed the inflector will be displaced radially inward over about 60 mm. This will vacate extra aperture to accommodate relocation of the stacked beam towards the centre of the ISR vacuum chamber thus permitting an increase of the stack dimensions due to multiple scattering with the residual gas at a pressure of  $10^{-9}$  torr during the beam lifetime.

To meet the vacuum requirement of  $10^{-9}$  torr, the magnet and its enclosing chamber must be degassed during bakeout at temperatures up to 300°C.

In order to minimize injection errors the tolerances imposed on the magnetic pulse form are:

Gradient on flat top	1%
Fast perturbations on flat top	$\pm 1\%$
and after 1 $\mu$ sec after flat top	

Maximum values are imposed on the remanent field and its gradient in the magnet gap as well as on the stray field and its gradient inside the metallic screen. These values are :

Remanent field	$10^{-3}$ T
Gradient of remanent field	$10^{-2}$ T/m
Pulsed stray field within screen	$10^{-3}$ T
Gradient of pulsed stray field within screen	$10^{-2}$ T/m

The requirements on the magnetic pulse form can be realized best with coaxial high voltage cables as pulse forming network (p.f.n.) and a lumped-constant delay-line type magnet. Table I gives the main parameters of the system for the case of 28 GeV/c protons. The maximum required operating voltage on the magnet is 21.5 kV.

Table I

Beam deflection angle	2.5 mrad
Total kick strength (28 GeV/c) protons	0.234 Tm
Number of magnet units	2
Total ferrite core length per magnet	1.2 m
Effective length of the magnet	1.37 m
Magnet gap width	44.5 mm
Electrical gap height	20 mm
Physical gap height (limited by 0.4 mm shims)	19.2 mm
Total inductance per magnet	$4.3 \times 10^{-6}$ H
Total capacitance per magnet	$22.0 \times 10^{-9}$ F
Characteristic impedance Z	14 $\Omega$
Filling time of magnet	0.31 $\mu$ sec
High Voltage on pulse forming network	38.6 kV
High voltage amplitude on magnet	19.3 kV
Stored energy in pulse forming network	63 J
Electrical pulse length	2.4 $\mu$ sec
Duty cycle	1 per sec (max)

#### Technical Description of ISR Inflector

Each of the two magnets of the inflector is housed in a separate, but interconnected, vacuum chamber and is energized independently by discharging a pulse forming network through the magnet into a matched termination resistance of 14  $\Omega$ . All the elements of the electrical circuit shown in Fig. 2 are of a matched coaxial form.

#### Mechanical Structure of Inflector

Figure 3 illustrates the magnet assembly and its support within the tank. The magnet assembly is 528 mm high by 218 mm wide by 1498 mm long. All metallic parts of the magnet structure are of titanium and the insulators are of alumina. The tanks, made from 304L stainless steel ( $\leq 0.03\%$  carbon), has an internal diameter of 0.625 m and a length of 1.96 m.

Essentially, the magnet is made up from 4 sub-sections, each containing 10 ferrite blocks 30 mm wide sandwiched between the titanium high voltage plates of the capacitor elements. The four sub-sections which are under mutual compression are held by 5 support plates by means of alumina oxide insulators. Three stiffening plates and four tension rods provide the necessary mechanical rigidity to the magnet.

The magnet is excited by one continuous high voltage conductor which is fixed tightly in the ferrite gap and provides the interconnection of the high voltage plates of the capacitors. The earthed return conductor plates are external to the ferrite gap. Being held by the support plates they form the base for the earth plates of the

capacitor elements. The separation between the earth and high voltage plates is 1.3 mm and they are vacuum insulated. Consequently, the plates are polished mechanically to achieve good high voltage keeping properties. A smooth, brilliant plate surface was achieved using a greaseless polishing compound of reducing grain size until the pore/ scratch depth was reduced to the specified  $\frac{1}{4}$  micro inch finish. A photograph of the magnet within its tank is shown in Fig. 4.

Bakeable and vacuum tight coaxial high voltage feedthroughs provide the interconnection between the magnet within the tank and the external electrical circuit. These are of a brazed construction with a hollow alumina cylinder, a molybdenum core and a titanium alloy outer ring to provide the gold ring vacuum seal interface.

Within its tank the magnet is suspended from two flat springs which permit differential thermal expansion between the magnet assembly and the stainless steel tank when the whole is being heated during bakeout.

In total the magnet weighs 330 kg, has a total plate area of 18 m<sup>2</sup> and a ferrite volume of  $15.5 \times 10^3$  cm<sup>3</sup>. Consequently, extreme cleanliness and care had to be exercised during its construction so that the outgassing rates could be kept within tolerable limits.

The pumping system of the prototype inflector setup - comprising one magnet tank unit and one empty tank - consists of a 500  $\ell$ /sec (effective) VacIon pump with a 70  $\ell$ /sec (effective) turbomolecular pump during the bakeout. After the bakeout, the turbomolecular pumping station was closed off from the tank and the VacIon pump was used with four 1000  $\ell$ /sec titanium sublimation pumps. These latter consist of 3 filaments per pump and each pump was activated by sublimating from one of its filaments for one minute each fourth day. This pumping capacity proved adequate to achieve final pressures of  $1 \times 10^{-10}$  torr while the magnet was being electrically pulsed in its tank.

Vacuum seals have been restricted to the copper gasket type except for the large diameter and non-standard flanges where gold wire seals are used.

#### Bakeout of Magnet Tank Assembly

Three bakeouts have now been completed with a prototype magnet tank assembly in its demountable 28 kW oven. The rate of temperature rise was dependent on the degassing rate of the system and its maximum value was 10°C/hour. This was also the normal rate of temperature fall. The peak temperature of 280°C was held for some 20 hours each time. No distortion of the magnet, nor of the tank has been discerned as a consequence of these bakeout cycles.

#### Electrical Characteristics

Coaxial high voltage cables are used as the pulse forming network, p.f.n., instead of a lumped-

parameter delay line, in order to generate the best possible rectangular current pulse. These cables are polyethylene insulated with copper inner and aluminium outer conductors; the inner diameter of the outer conductor being 53 mm. In order to reduce the resistive losses of the cables as well as the electrical stress in the cable insulation 2x28  $\Omega$  cables have been used in preference to a single 14  $\Omega$  cable. No semi-conducting screens adjacent to the cable conductors have been applied as these increase the resistive losses by a large factor.

The cables have been factory tested at 60 kV amplitude at 50 Hz alternating voltage and they have subsequently endured  $10^7$  pulses at 50 kV under normal operating conditions. The measured impedance value was within the specified tolerance  $\Delta Z/Z = \pm 1\%$  at 1 MHz, the attenuation has been measured to be 0.44 db/100 metres at 20 MHz for the 28  $\Omega$  cables.

English Electric Type CX 1168 double gap deuterium filled tetrode thyratrons rated at 80 kV have been employed as switches rather than maintenance prone spark gaps and have demonstrated excellent trouble free characteristics in this application.<sup>3</sup>

Under test conditions, these valves have switched up to 60 kV (on the charging line) into a 14  $\Omega$  load. Tests at 50 kV simulating the inflector mode of operation have given the following results. Risetimes are variable between 30 and 100 nsecs depending upon voltage setting of reservoir heater, i.e. anode rates of current rise of between 60 kA/ $\mu$ sec and 18 kA/ $\mu$ sec are attainable. Under these latter conditions, a lifetest of more than  $10^7$  pulses of 2.4  $\mu$ secs long - at pulse repetition rates up to 4 per second - has been completed. During this, the jitter was  $\pm 1$  nsec and long term anode delay drift was less than  $\pm 5$  nsecs when a stabilized power supply was employed for the cathode and reservoir heaters.

A 14  $\Omega$  'Morganite' solid carbon resistor, housed in a coaxial chamber, is used as the termination of the electrical circuit. This is temperature controlled by means of an oil circulation system which, besides acting as an energy sink, provides the means through heating or cooling of regulating the resistance value for minimal electrical pulse reflections.

14  $\Omega$  polyethylene coaxial cables are used for the interconnections between the thyatron, magnet and terminating resistor.

#### Magnet Performance and Results

After the bakeout and under ultra high vacuum, the magnet was high voltage conditioned using the 2.4  $\mu$ sec long pulses from the p.f.n. A total of 3 m<sup>2</sup> of titanium plate surface with a separation of 1.3 mm is subjected to electrical stress during pulsing in each magnet. The choice of titanium for the capacitor plates was based on its reported<sup>4</sup> good voltage keeping characteristic as well as on

independent tests carried out in our laboratory.

Initially, high voltage breakdown of the gap is associated with dust and plate scratches. Spark condition rate proves to be erratic but rapid in the high voltage range up to 18 kV. After this had been passed, conditioning was effected by pulsing 500 volts below the breakdown threshold until a new threshold could be established. In this manner a working voltage of 21.5 kV was established at a rate of rise of about 1 kV per  $10^4$  pulses from 18 kV upwards. At this level a life-test of  $10^7$  pulses was concluded with the spark breakdown rate reducing rapidly from about 1 per  $10^4$  pulses to zero.

After the lifetest, the magnet plates were further conditioned to 25 kV and  $1.5 \times 10^6$  pulses were made without breakdown. This level was easily re-established even after dry nitrogen had been admitted to the tank and after the magnet had been removed into the laboratory atmosphere.

The method of pulse conditioning suffers from the disadvantage that in the event of a breakdown, the whole line energy (68 J at 20 kV) is dissipated in the plate at the point of breakdown, which is sufficient to destroy the plate surface at that point.

Direct current conditioning has not, so far, been employed since it has not proven necessary. This technique is not necessarily more straightforward than the pulsing method since both insulators and vacuum insulated gaps will breakdown at lower voltages under constant potential than would be the case for fast pulses.

It had previously been demonstrated on a 1/4 length model that spark conditioning of the titanium plates was hazardous but that the pre-breakdown phenomena for pulses of 2.4  $\mu$ secs long could be exploited to achieve conditioning. The better high voltage breakdown characteristic of the titanium alloy with 6% aluminium 4% vanadium has been shown to be insignificant in this application, where surface area, polishing and cleaning are the obvious limiting factors.

#### Magnetic Field and its Distribution

For measurement of the magnetic field distribution, a matched 2 mm wide single turn magnetic field probe of 1.6 m length has been used and its output pulse compared with the electrical pulse from the p.f.n. This difference method has afforded a precision better than 2% for the measurements of the lateral field distribution in the gap. Figure 5 shows the magnetic field pulse measured within the gap from which it can be seen that the flat top gradient is less than the specified 1% when the gradient of 0.5% due to the integrator time constant - 500  $\mu$ secs - is subtracted. The fast perturbations due to system mismatch have been measured to be within the specified  $\pm 1\%$  of peak value both on the flat top and 1  $\mu$ second afterwards.

The transverse magnetic field distribution

within the gap is shown in Fig. 6. Curves 2 and 3 of this figure represent the distribution for  $9.95 \times 10^{-2}$  T, corresponding to 22.5 kV on the magnet, with the screen closed and open respectively, and line 1 the distribution for  $2.21 \times 10^{-2}$  T, corresponding to 5 kV with the screen closed. The nominal values of magnetic induction stated here refer to the centre of gap position. This range covers the foreseeable demands on the fast inflector. The nominal working point for 28 GeV/c protons will be  $8.55 \times 10^{-2}$  T for 19.3 kV on the magnet.

We consider as an example a useful field region with a magnetic field deviation of  $\pm 4\%$  at 41.5 mm in the inflector gap. On the nominal deflection angle of 2.5 mrad this corresponds to an error of  $\pm 0.1$  mrad and for the extreme case of a beam of 40 mm full width extending up to this point the increase of the horizontal dimension would be 0.8 mm. This would correspond to a 4% increase in the emittance of the injected beam. It should be noted that this error is only applicable to the lateral extremity of the beam, which corresponds to the part of the beam with minimum angle of their betatron oscillations.

Figure 6 shows that the useful field region extends over 41.5 mm at a magnetic induction of  $9.95 \times 10^{-2}$  T, with no reduction at  $2.2 \times 10^{-2}$  T. This has been achieved using shims of 0.4 mm high and 6 mm wide along the ferrite pole edges and has been further enhanced by the field concentration at the edges due to the proximity of the screen - compare lines 2 and 3. Over the useful gap aperture, the maximum field gradient is about  $5 \times 10^{-2}$  T/m. This can be partially corrected with the quadrupole magnets of the beam transfer system.

Within the screen, the maximum field (corresponding to  $9.95 \times 10^{-2}$  T in the gap) is  $5 \times 10^{-4}$  T with a gradient of  $5 \times 10^{-3}$  T/m. These values are proportional to the gap field.

The magnetic field at gap centre versus the pulsed high voltage has been measured to be linear to within 1% for the range 5 to 22.5 kV.

To minimize the effects due to remanence, a low coercivity ferrite (Philips 4A1) has been chosen for the core. The lower saturation point of this ferrite is not limiting in this application. The remanent field in the gap is  $3.5 \times 10^{-4}$  T with a maximum gradient of  $7 \times 10^{-3}$  T/m.

#### Conclusion

These results show that the precise magnetic pulse form required for injection of protons into the ISR can be obtained with an available useful field region in excess of 40 mm.

The reliability of the total inflector system has been proven since all p.f.n. elements and the magnet have been operated at the maximum required operating voltage of 21.5 kV for over  $10^7$  pulses which we estimate to equal several years of ISR utilization. The whole system has further

operated at 25 kV for  $1.5 \times 10^6$  pulses without difficulties.

The bulk and complex structure of the magnet has been proven to be not limiting for ultra high vacuum requirements.

At the present time 5 further magnets of the same design are under construction, 4 of these will be commissioned and installed in the ISR tunnel during September of this year.

#### Acknowledgements

It is a pleasure to acknowledge the encouragement given to us in this work by our Group Leader, Dr. B. de Raad, the able assistance of our colleague J.P. Zanasco, and the support of our technicians A. Jaeger and G. Losch.

#### References

- 1) The Design Study of Intersecting Storage Rings for the CERN Proton Synchrotron, CERN AR/Int. SG/64-9.
- 2) W. Schnell: "Stacking with Missing Buckets, another way of gaining the ISR/PS circumference factor". CERN-RF/66-35 (1966).
- 3) H. O'Hanlon and J.P. Zanasco: "A high voltage Thyatron Switch for the Fast Inflector of the ISR". CERN ISR-BT/67-55 (1967).
- 4) J. Huguenin and R. Dubois: "Measurements on a high gradient accelerating tube model. Investigations of the properties of Titanium Electrodes". CERN MPS Div. CERN 65-23 (1965).

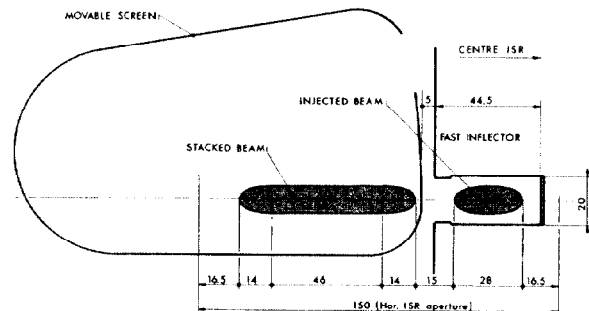


Fig. 1 Injected and Stacked Beam Sizes in ISR

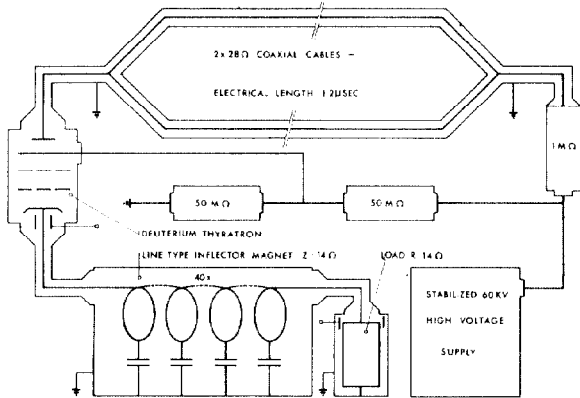


Fig. 2 Electric Circuit of ISR Inflector

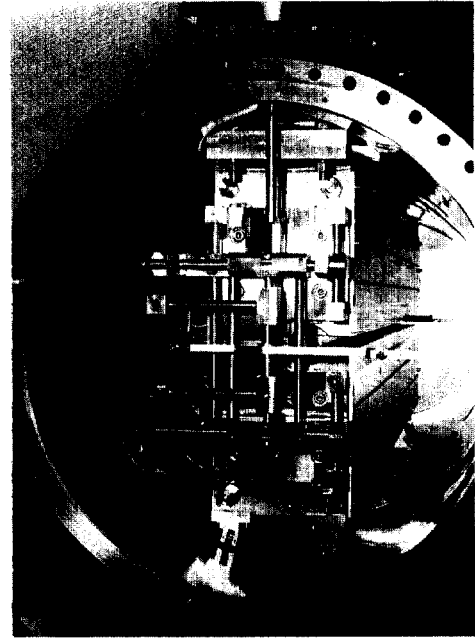


Fig. 4 Inflector Magnet mounted in its UHV Tank. A scanning machine for making magnetic measurements is temporarily mounted onto the magnet.

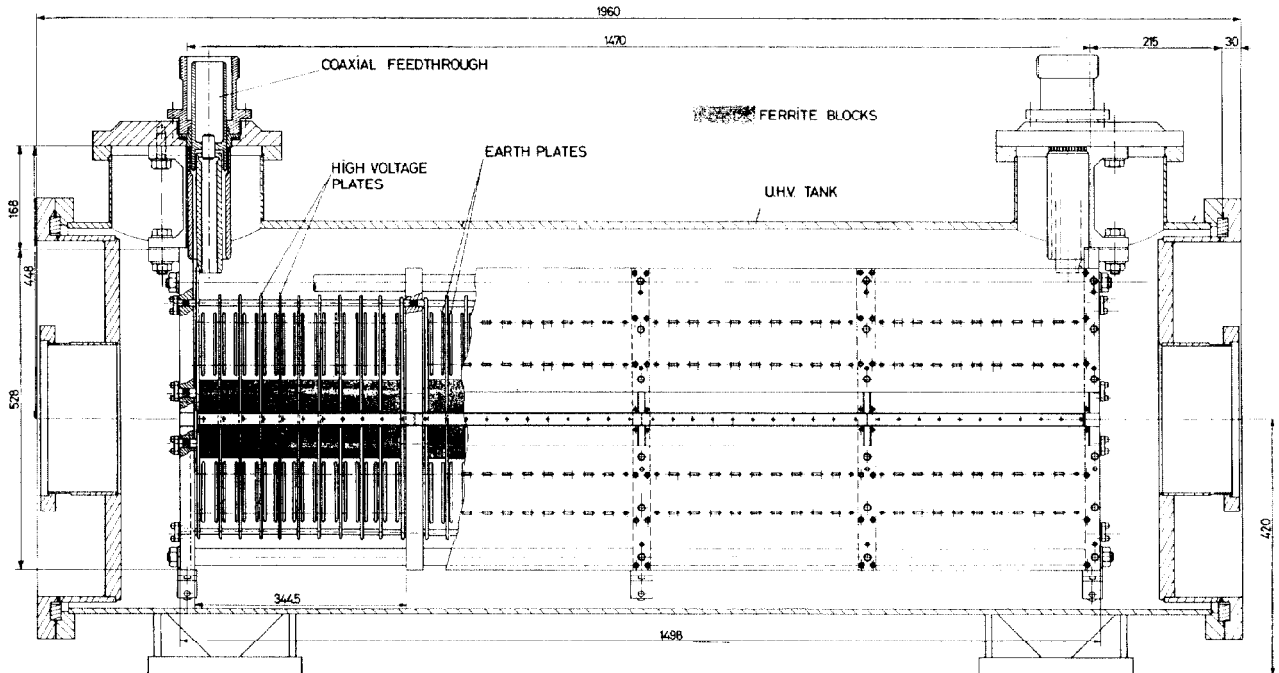


Fig. 3 Inflector Magnet and Ultra-High Vacuum Tank Assembly

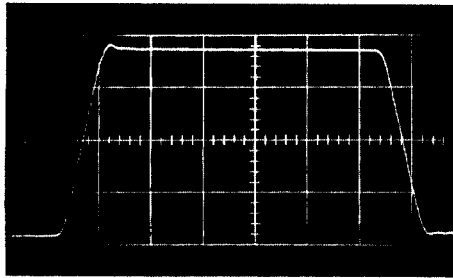


Fig. 5 Magnetic Field Pulse Form.  
 Time-base 400 nsecs/div.  
 Integrator time constant 500  $\mu$ secs.

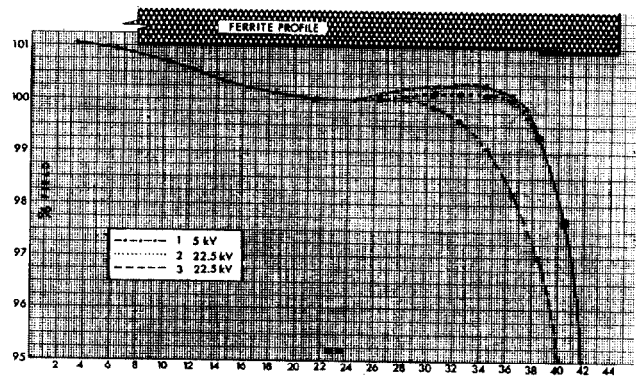


Fig. 6 Transverse Field Distribution in median plane of the gap of the magnet.